Sudden death and sudden birth of quantumness for a harmonic oscillator interacting with a classical fluctuating environment

Jacopo Trapani and Matteo Bina
Dipartimento di Fisica dell'Università degli Studi di Milano, I-20133 Milano, Italia

Sabrina Maniscalco
Turku Centre for Quantum Physics, Department of Physics and Astronomy, University of Turku, FI-20014 Turun yliopisto, Finland

Matteo G. A. Paris
*Dipartimento di Fisica dell'Università degli Studi di Milano, I-20133 Milano, Italia and CNISM, Udr Milano, I-20133 Milano, Italy.**

(Dated: March 18, 2015)

We address the dynamics of nonclassicality for a quantum system interacting with a noisy fluctuating environment described by a classical stochastic field. As a paradigmatic example, we consider a harmonic oscillator initially prepared in a maximally nonclassical state, e.g. a Fock number state or a Schrödinger cat-like state, and then coupled to either resonant or non-resonant external field. Stochastic modeling allows us to describe the decoherence dynamics without resorting to approximated quantum master equations, and to introduce non-Markovian effects in a controlled way. A detailed comparison among different nonclassicality criteria and a thorough analysis of the decoherence time reveal a rich phenomenology whose main features may be summarized as follows: i) classical memory effects increase the survival time of quantum coherence; ii) a detuning between the natural frequency of the system and the central frequency of the classical field induces revivals of quantum coherence.

PACS numbers: 03.65.Yz, 03.65.Ta, 03.65.Xp

arXiv:1411.0946v2 [quant-ph] 17 Mar 2015

I. INTRODUCTION

The environment-induced decoherence is the prevailing explanation for the loss of nonclassicality of an open quantum system, being responsible for the relaxation of the system to a statistical mixture of classical-like states [1–3]. In this framework, a non-zero temperature environment is usually described in terms of a quantized ensemble of simple physical systems, e.g. harmonic oscillators or spins, spanning a wide frequency range and interacting with the quantum system of interest through a suitable interaction Hamiltonian. A set of approximations, such as Born and Markov approximations, is then exploited to obtain a differential master equation describing the dissipative dynamics of the open quantum system [4–10].

In a Markovian approach, the environment time-correlation functions are assumed to decay istantaneously compared to the typical time-scale of the system, i.e. memory effects have no influence on the system dynamics. In this context, a thoroughly studied quantum system is the single-mode quantum harmonic oscillator interacting with a bosonic bath of oscillators. For such an open system, the decoherence time, ruling the transition from the quantum to the classical regime, may be identified by different nonclassicality criteria, which have been widely investigated [11–24] and compared [25]. Extensions to multimode systems [26–29] have been analyzed, and the decoherence process has been addressed extensively [30, 31]. Besides the fundamental interest, the analysis of the quantum-to-classical transition has relevant applications in the field of quantum technology. In fact, the generation and detection of nonclassical states is often a prerequisite to generate entanglement and discord for quantum information purposes in all-optical setups [32–37].

The assumption of weak coupling between the system and its environment, i.e. the Born approximation, is valid for a wide class of systems. On the other hand, the Markov assumption, is violated in several situations of interest, e.g. in biological, optical, or solid-state systems [38–41], where a more detailed description of the environment, including the spectral structure and the inherent memory effects, is required [42–45]. In this regime, decoherence may be less detrimental, and the dynamics may even induce *re-coherence*. For this reason a great attention has been devoted to the study of the corresponding non-Markovian dynamics in different systems ranging from quantum optics to mechanical oscillators and harmonic lattices [46–54]. Besides, there are evidences that non-Markovian open quantum systems [55–59] can be useful for quantum technology [60–62].

There are two main paradigms to describe the dynamics of open quantum systems: on the one hand, as mentioned above, one may look at system and enviroment as a single global quantum system whose evolution is governed by an overall unitary operator. Upon tracing out the environment' degrees of freedom, we then obtain the dynamics of the system. On the other hand, we may consider the open quantum system under the action of external random forces, i.e. coupled to a stochastic classical field. Here the partial trace is substituted by the average over the different realizations of the stochas-

*matteo.paris@fisica.unimi.it

tic field. While the system-enviroment approach is more fundamental in nature, the approximations employed to achieve manageable dynamical equations often precludes a detailed description of the dynamics. Indeed, systems of interest for quantum technology generally interact with complex environments, with many degrees of freedom, and a fully quantum description may be challenging or even unfeasible. In these situations, classical stochastic modeling of the environment represents a valid and reliable alternative. In fact, it has been shown that for certain system-environment interactions a classical description can be found that is completely equivalent to the quantum description [63–66]. Besides, there are various experimental evidences that many quantum systems of interest interact with classical forms of noise, typically Gaussian noise [67–69].

In this paper, we consider the paradigmatic case of a quantum harmonic oscillator coupled to a classical stochastic field (CSF) [70]. Here, the advantage of choosing a CSF description for the environment is twofold: on the one hand stochastic modeling allows us to describe the decoherence dynamics without resorting to approximated quantum master equations. On the other hand, we may introduce non-Markovian effects in a controlled way. For qubit systems, description of environment-induced decoherence by the interaction with classical fluctuacting field has been successfully carried out [71–80].

We will assume that the harmonic oscillator is initially prepared in a maximally nonclassical state, e.g. a Fock number state or a superposition of (possibly mesoscopic) coherent states, the so-called *Schrödinger-cat* state, and perform a detailed comparison of the decoherence times according to four different criteria for nonclassicality: the nonclassical depth [20], the negativity of the Wigner function [81] the Vogel criterion [17], based on the characteristic function, and the Klyshko criterion for the photon number distribution [14]. While the sole nonclassical depth criterion represents a proper (i. e. necessary and sufficient) criterion for nonclassicality, the other quantities have the advantage of being good candidates for an experimental implementation.

Our results show that according to all the quantifiers of nonclassicality, the presence of time correlations (i.e. memory effect) in the classical environment enhances the *survival time* of, say, the Schrödinger cat state, i.e. it preserves coherence for a longer time compared to the Markovian case. Furthermore, these memory effects become more and more important as far as the central frequency of the stochastic field is detuned with respect to the natural frequency of the harmonic oscillator, up to inducing sudden death and sudden birth of quantumness, i.e. collapse and revival of quantum coherence.

The paper is organized as follows: in Sec. II we introduce the system under investigation and the stochastic modeling of the environment, as well as the details of the system-environment interaction. We also describe the initial preparation of the system, discuss their nonclassicality and introduce and all the figures of merit used in the subsequent Sections. In Section III we address in details the decoherence dynamics of the system interacting with a classical environment described by the Ornstein-Uhlenbeck process. We also evaluate the input-output fidelity of the corresponding quantum channel and discuss its use as a potential indicator of non-Markovianity in our system. In Section IV, we briefly analyze the decoherence dynamics for an environment described by a CSF with a power-law autocorrelation function. Finally, Section V closes the paper with some concluding remarks.

II. THE SYSTEM

We consider a quantum harmonic oscillator interacting with a classical external field. The Hamiltonian of the system may be written as $H = H_0 + H_{SC}$ where the free and interaction Hamiltonians are given by

$$H_0 = \hbar\omega_0 a^\dagger a \tag{1}$$

$$H_{SC} = \hbar\left[a\bar{B}(t)e^{i\omega t} + a^\dagger B(t)e^{-i\omega t}\right], \tag{2}$$

with ω_0 the natural frequency of the oscillator and $B(t)$ a time-dependent fluctuating field with central frequency ω described by a stochastic process with zero mean, whose complex conjugate is $\bar{B}(t)$. From now on and throughout the paper, we will consider the Hamiltonian H rescaled in units of $\hbar\omega_0$. As a straightforward consequence, the stochastic classical field $B(t)$, its central frequency ω and the time t become dimensionless quantities (in units of ω_0 and ω_0^{-1} respectively).

We assume that the system is initially prepared in a Fock state $|n\rangle$ or in a superposition of coherent states with opposite phases, the so-called Schrödinger-cat state $|\psi_{cat}\rangle = \mathcal{N}^{-\frac{1}{2}}\left(|\alpha\rangle + |-\alpha\rangle\right)$ where $|\alpha\rangle$ indicates a coherent state and the normalization constant is $\mathcal{N} = 2\left[1+\exp(-2|\alpha|^2)\right]$. We focus on Fock or cat states since they have maximal nonclassical depth and thus represent the proper preparation to analyze the quantum-to-classical transition in full details. Actually, as we will show in the next paragraph, any pure state other than Gaussian pure states would be equally good to address the dynamics of the nonclassical depth. On the other hand, sufficient criteria as the Vogel criterion and the Klyshko criterion do depend on the specific state under investigation, and thus having in mind a specific class of states will be of help to properly address the detection of nonclassicality in realistic conditions.

The nonclassical depth η of a quantum state [20] is a quantitative measure of its nonclassicality, and is defined as the minimum number of photons to be added to a state in order to erase all of its quantum features. In terms of the s-ordered Wigner functions, the nonclassical depth is given by

$$\eta = \frac{1}{2}(1-\bar{s}),$$

where $\bar{s}$ is the largest value of s for which the corresponding s ordered Wigner function $W_s[\rho](\alpha)$ is positive and may be seen as a classical probability distribution. In turn, we have $0 \leq \eta \leq 1$. The s-ordered characteristic function and the s-ordered Wigner function for the Fock states $|n\rangle$ and the cat states $|\psi_{cat}\rangle$, as well as the cat's matrix elements in the Fock basis, are given in Appendix A. As it is apparent from their expressions, the s-ordered Wigner functions of both classes

of states are not positive function for any $-1 < s \leq 1$. Correspondingly, the nonclassical depth η of a Fock or cat state is equal to one [15] independently on α or n, i.e. the cat and the number states are maximally nonclassical states independently on their energy, as the first positive Wigner function corresponds to $s = -1$, i.e. the Husimi Q function. More generally, we have that the nonclassical depth is $\eta = 1$ [21] for any pure state other than Gaussian pure states (squeezed coherent state); squeezed states have $0 \leq \eta \leq \frac{1}{2}$ depending on the squeezing parameter, while coherent state have $\eta = 0$, properly capturing the fact that they are the closest analog to classical states for the quantum harmonic oscillator.

The Hamiltonian in the interaction picture reduces to:

$$H_I(t) = a e^{-i\delta t}\bar{B}(t) + a^\dagger e^{i\delta t} B(t) \tag{3}$$

where $\delta = 1-\omega$ is the detuning between the natural frequency of the oscillator and the central frequency of the CSF (in units of ω_0). The corresponding evolution operator is given by

$$U(t) = \mathcal{T} \exp\left\{-i\int_0^t ds\, H_I(s)\right\}, \tag{4}$$

where $\mathcal{T}$ denotes time ordering. Notice, however, that as far as $B(t_1)\bar{B}(t_2) = [B(t_1)\bar{B}(t_2)]^*$, the two-time commutator $[H_I(t_1), H_I(t_2)]$ is proportional to the identity

$$[H_I(t_1), H_I(t_2)] = 2\, i \sin\left[\delta(t_2 - t_1)\right]\; B(t_1)\bar{B}(t_2)\, \mathbb{I}\,, \tag{5}$$

and this form allows to evaluate time ordering using the Magnus expansion [84, 85], which results to be exact already at the second order. According to the Magnus expansion, the evolution operator may be written as

$$U(t) = \exp(\Omega_1 + \Omega_2) \tag{6}$$

where:

$$\Omega_1 = -i\int_0^t ds_1\, H_I(s_1) = a^\dagger \phi_t - a\phi_t^* \tag{7}$$

$$\phi_t = -i\int_0^t ds_1\, e^{i\delta s_1} B(s_1) \tag{8}$$

and

$$\Omega_2 = \frac{1}{2}\int_0^t ds_1 \int_0^{s_1} ds_2\; [H_I(s_1), H_I(s_2)] \propto \mathbb{I}. \tag{9}$$

Since Ω_2 is proportional to the identity we may write the evolution of an initial density operator $\rho(0)$ as

$$\rho(t) = \left[e^{\Omega_1}\rho(0)\, e^{\Omega_1^*}\right]_B = \left[D(\phi_t)\rho(0)D^\dagger(\phi_t)\right]_B \tag{10}$$

where $D(\mu) = e^{\mu a^\dagger - \bar{\mu} a}$ is the displacement operator and $[\dots]_B$ denotes the average over the different realization of the stochastic process. Eq. (10) shows that the interaction Hamiltonian with a classical field results in a time-dependent displacement of argument ϕ_t, related to the classical field $B(t)$ and, then, strongly affected by its stochasticity.

In our system we assume that the CSF $B(t) = B_x(t) + iB_y(t)$ is described by a Gaussian stochastic process with zero mean $[B_x(t)]_B = [B_y(t)]_B = 0$ and diagonal structure of the autocorrelation matrix

$$[B_x(t_1)B_x(t_2)]_B = [B_y(t_1)B_y(t_2)]_B = K(t_1, t_2) \tag{11}$$

$$[B_x(t_1)B_y(t_2)]_B = [B_y(t_1)B_x(t_2)]_B = 0, \tag{12}$$

with (dimensionless) kernel autocorrelation function $K(t_1, t_2)$.

Using the Glauber decomposition [13] for the initial state

$$\rho(0) = \int \frac{d^2\mu}{\pi}\, \chi_0[\rho(0)](\mu)\, D^\dagger(\mu)\,, \tag{13}$$

where the (symmetrically ordered) characteristic function is given by $\chi_0[\rho](\mu) = \mathrm{Tr}[\rho\, D(\mu)]$, we may write the evolved state as

$$\rho(t) = \int \frac{d^2\mu}{\pi}\, \left[e^{\mu\phi^*(t) - \mu^*\phi(t)}\right]_B \chi_0[\rho(0)](\mu) D^\dagger(\mu)\,, \tag{14}$$

where, for any Gaussian stationary process, we may write

$$\left[e^{\mu\phi^*(t) - \mu^*\phi(t)}\right]_B = e^{-|\mu|^2\sigma(t)} \tag{15}$$

and $\sigma(t)$ (following Ref. [83]) can be expressed as

$$\sigma(t) = \int_0^t\int_0^t ds_1 ds_2\, \cos\left[\delta(s_1 - s_2)\right]\, K(s_1, s_2)\,. \tag{16}$$

The s-ordered characteristic function $\chi_s[\rho(t)](\mu)$ of the evolved state is given by

$$\chi_s[\rho(t)](\mu) = \chi_0[\rho(0)](\mu)\, e^{\frac{1}{2}|\mu|^2[s - 2\sigma(t)]}\,, \tag{17}$$

which corresponds to a Gaussian noise channel [11, 88]:

$$\rho(t) = G[\rho(0)] = \int \frac{d^2\gamma}{\pi\sigma(t)} e^{-\frac{|\gamma|^2}{\sigma(t)}}\, D(\gamma)\rho(0)\, D^\dagger(\gamma), \tag{18}$$

where $\sigma(t)$ in Eq. (16) plays the role of the variance of the Gaussian channel.

In order to obtain quantitative results we focus on Ornstein-Uhlenbeck (OU) process [70, 82], with autocorrelation function given by

$$K(t_1, t_2) = \frac{1}{2}\lambda\gamma\, e^{-\gamma|t_1 - t_2|}\,. \tag{19}$$

The main conclusions of our analysis, however, are independent on the specific feature of the process, as far as we consider classical fields described by stationary Gaussian processes. In Eq. (19) λ is a coupling constant and γ is a memory parameter equal to the inverse of the characteristic time of the environment (in units of ω_0). As we will show in the following Sections the memory effects associated to the interaction with a classical OU field allows the initial state to preserve its nonclassicality for times longer than those achieved with a Markovian environment. As we will see, the smaller is γ,

the longer is the survival time of quantumness at fixed values of the detuning δ. Conversely, for $\gamma \gg 1$, the survival time of the cat approaches the Markovian values [25]. Indeed, for $\gamma \gg 1$ the autocorrelation function in Eq. (19) approaches a Dirac delta function.

For the OU process $\sigma(t)$ may be explicitly written as

$$\sigma(t) = \frac{\lambda\gamma}{(\gamma^2+\delta^2)^2}\Big\{\delta^2(1+t\gamma) - \gamma^2(1-\gamma t) + e^{-\gamma t}\Big[(\gamma^2-\delta^2)\cos\delta t - 2\gamma\delta\sin\delta t\Big]\Big\} \qquad (20)$$

leading to the following approximated expressions in some particular regimes:

$$\sigma(t) \simeq \lambda t + \frac{\lambda}{\gamma}\, e^{-\gamma t}\cos\delta t \qquad \gamma \gg 1 \quad (21)$$

$$\sigma(t) \simeq \frac{\lambda\gamma}{\delta^2}(1-\cos\delta t) \qquad \gamma \ll 1, \delta \gg 1 \quad (22)$$

$$\sigma(t) \simeq \frac{\lambda\gamma t^2}{2}(1-\delta^2 t^2) \qquad \gamma \ll 1, \delta \ll 1\,. \quad (23)$$

Overall, the interaction with a classical environment corresponds to a Gaussian channel with the time-dependent width $\sigma(t)$, which fully characterizes the dynamics.

Finally, we notice that the map in Eq. (18) is a solution of the standard Born-Markov quantum optical master equation

$$\frac{d}{dt}\rho(t) = \frac{\Gamma}{2}(N+1)[2a\rho(t)a^\dagger - a^\dagger a\rho(t) - \rho(t)a^\dagger a] + \frac{\Gamma}{2}N[2a^\dagger\rho(t)a - aa^\dagger\rho(t) - \rho(t)aa^\dagger] \qquad (24)$$

in the limits $N \gg 1$ and $\Gamma t \ll 1$, where N is the number of thermal photons in the environment and Γ the dissipation rate. Eq. (24) describes the open-system dynamics of a harmonic oscillator (weakly) interacting with a Markovian bath of harmonic oscillators at the temperature $[\log(1+N^{-1})]^{-1}$. In other words, in the regime of high temperature and short times, the interaction with a quantized environment is equivalent to the interaction with a classical stochastic field. The explicit mapping is provided by the relation $\sigma(t) \longleftrightarrow \Gamma N t$. Further insight about the meaning of the involved parameters may be gained using a short-time, detuning-independent, approximation for $\sigma(t) \simeq \frac{1}{2}\lambda\gamma t^2$.

III. DYNAMICS OF QUANTUMNESS

In this Section we address in details the quantum-to-classical transition, according to four different criteria, for a Schrödinger cat and a Fock state interacting with a CSF. We evaluate the decoherence times and analyze whether and how these may increase for a channel with memory, compared to a Markovian one. We also discuss the role of detuning in producing collapse and re-coherence effects (sudden death and birth of quantumness).

A. Nonclassical depth

As mentioned above, the nonclassical depth was introduced as the minimum number of thermal photons needed to erase the quantum features of a given state [20]. In the phase space, the nonclassical depth enters as the minimum width of the Gaussian convolution needed to transform the (possibly singular) Glauber P function of a given state into a positive function. According to this measure, Fock number states and Schrödinger-cat states are maximally nonclassical states independently on their energy.

Accordingly, the spirit of the nonclassical depth criterion is to find the smallest interaction time t_Q such that the P-distribution of the evolved state becomes positive, i.e. the evolved state is a statistical mixture of coherent states. Indeed, the nonclassical depth criterion well captures the intuition of decoherence as relaxation of the system into a statistical mixture of classical states.

As we will see, the interaction with the CSF turns the initial P distribution into a positive function after a finite interaction time t_Q. In addition, depending on the value of the dimensionless parameters λ, γ and δ we may also observe revivals of coherence (sudden birth of quantumness). In order to determine these thresholds, one should consider the evolved state $\rho(t)$ and evaluate the time-dependent value of the nonclassical depth. Actually, it is sufficient to evaluate the nonclassical depth only for the initial state since Eq. (17) shows that the normally-ordered characteristic function $\chi_1[\rho(t)](\mu)$ (which generates the P distribution) corresponds to the $\tilde{s}$-ordered characteristic function of the initial cat state $\chi_{\tilde{s}}[\rho(0)](\mu)$, where $\tilde{s} = [1-2\sigma(t)]$. As the nonclassical depth of the cat or the Fock states is equal to one, the P distribution becomes positive when it turns into a Husimi Q function, which corresponds to $\tilde{s} = -1$. This happens in a finite (dimensionless) time t_Q that is straightforwardly defined by

$$\sigma(t_Q) = 1. \qquad (25)$$

For values of t such that $\sigma(t) > 1$, the P distribution is a positive function and the state is classical. It is worth noticing that the nonclassical depth criterion only depends on $\sigma(t)$, which is indipendent on the initial state parameter α or n. More generally, for a state with initial nonclassical depth η_0 the decoherene time t_Q is given by the solution of the equation $\sigma(t_Q) = \eta_0$.

Let us firstly focus on the resonant interaction ($\delta = 0$). In this case $\sigma(t)$ reduces to:

$$\sigma(t) = \lambda t + \frac{\lambda}{\gamma}\left(e^{-\gamma t} - 1\right), \qquad (26)$$

and the equation $\sigma(t) = 1$ has a single solution for any pairs of values of λ and γ. We thus have sudden death of quantumness without any revival. As we anticipated in the previous Section, the autocorrelation function of the process approches a Dirac delta in the limit of large γ. If we perform the limit at this stage we obtain $\lim_{\gamma\to\infty}\sigma(t) = \lambda t$. This form of $\sigma(t)$ coincides with that obtained using Eq. (24) and assuming that $\lambda = \Gamma N$. In other words, the limit $\gamma \gg 1$ leads to the Markovian regime. This also confirms the idea that γ plays the role

of a memory parameter. More explicitly, its inverse set the time for which the field correlations cease to be significative. Large values of γ describes environments with no memory of their previous configurations. In the Markovian limit the decoherence time $t_Q^{(M)}$ is given by:

$$t_Q^{(M)} = \frac{1}{\lambda} = \frac{1}{\Gamma N}. \tag{27}$$

In the present non-Markovian case, we have

$$t_Q = \frac{\gamma+\lambda}{\gamma\lambda} + \frac{1}{\gamma}\,\xi\left(-e^{-1-\gamma/\lambda}\right),$$

where $\xi(x)$ is the product-log function, i.e. the positive real solution y of the equation $x = ye^y$. Using this expression, it is possible to show numerically that $t_Q > t_Q^{(M)}$ for any value of γ and λ, i.e. the non-Markovian character of the field preserves the initial nonclassicality for longer times compared to the Markovian case. This is illustrated in the left panel of Fig. 1 where we show the ratio $t_Q/t_Q^{(M)}$ as a function of γ for different values of λ: the ratio is larger than unity for any value of γ and it increases for increasing λ, i.e. nonclassicality is better preserved for larger coupling. For increasing γ, the decoherence time t_Q goes to the Markovian value independently on the value of the coupling.

Let us now analyze what happens if we turn on the detuning between the natural frequency of the system and the central frequency of the field. In this case the equation $\sigma(t) = 1$ may have more than one solution (fixing all the parameters δ, γ and λ) and thus revivals of coherence may appear. In the right panel of Fig. 1 we show the contour plots $\sigma(t_Q) = 1$ as a function of time and γ for different values of the detuning δ and for a fixed value $\lambda = 1$ of the coupling. The regions lying to the right of the curves correspond to $\sigma(t) > 1$, i.e. classicality (CL), whereas regions of nonclassicality (NCL) $\sigma(t) < 1$ lie to the left. There are two main effects: i) at fixed γ the decoherence time t_Q increases with the detuning, the effect is more pronounced for smaller γ; ii) revivals of quantumness, i.e. sudden death followed by sudden birth of quantumness, appear at fixed (and not too large) values of γ. This is illustrated in the right panel of Fig. 1 and in the corresponding inset, where, for $\delta = 0.3$ (solid red line) and $\gamma = 0.05$, $\sigma(t)$ displays re-coherence effects. Notice also that for increasing γ, revivals disappear and t_Q becomes more and more independent on the detuning, thus further confirming that for large γ we are approaching the Markovian limit.

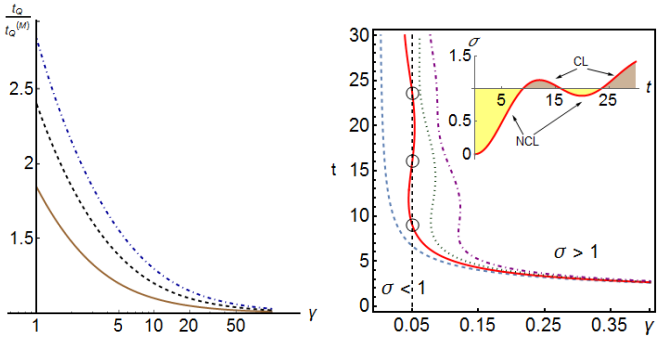

FIG. 1: (Color Online) Dynamics of quantumness according to the nonclassical depth criterion. Left panel: dimensionless decoherence time t_Q for a resonant interaction as a function of the memory parameter γ, for different values of the coupling $\lambda = 1$ (solid brown), $\lambda = 2$ (dashed black) and $\lambda = 3$ (dot-dashed blue). For $\gamma \to \infty$, t_Q approaches the Markovian limit $t_Q^{(M)}$ independently on λ. Right panel: contour plots of $\sigma(t_Q) = 1$, in the off-resonance case, as a function of γ for a fixed value of the coupling $\lambda = 1$ and different values of the detuning $\delta = 0.3$ (solid red), $\delta = 0.4$ (dotted green) and $\delta = 0.5$ (dot-dashed purple). The dashed blue curve is chosen as a reference for the resonant case $\delta = 0$. In the regions lying to the left of the curves we have $\sigma(t) < 1$, i.e. nonclassicality. The vertical line (dashed black) denotes points at fixed $\gamma = 0.05$ and the black circles indicate the three solutions of $\sigma(t_Q) = 1$ for $\delta = 0.3$. Correspondingly, the regions of nonclassicality (NCL) and classicality (CL) are highlighted in the inset.

B. Wigner negativity

A different notion of nonclassicality is based on the negativity of the Wigner function which is never singular, but it can take on negative values for nonclassical states, such as Fock states or superposition of coherent states[19]. The notion of nonclassicality arising from the negativity of the Wigner function is not equivalent to the nonclassical depth and it has been linked to non-local properties [86, 87]. Indeed, squeezed vacuum states display a positive Wigner function even though their nonclassical depth range from $\eta = 0$ to $\eta = \frac{1}{2}$, increasing with energy.

We can evaluate the time t_W in which the P function turns into a Wigner function in the very same way we evaluated the nonclassical depth time in the previous section. The condition that t_W must satisfy, in order to change from a normally ordered into a symmetrically ordered characteristic function, is

$$\sigma(t_W) = \frac{1}{2}. \tag{28}$$

Exactly as the nonclassical depth criterion, the Wigner decoherence time depends only on $\sigma(t)$ and it is not affected by the initial state parameter α or n. For a state with initial nonclassical depth equal to η_0, the Wigner decoherence time is the solution of $\sigma(t_W) = \eta_0 - 1/2$ if $\eta_0 > \frac{1}{2}$ or $t_W = 0$ otherwise.

In the Markovian limit $\gamma \gg 1$ the decoherence time $t_W^{(M)}$ of the cat or the Fock state is simply half of $t_Q^{(M)}$

$$t_W^{(M)} = \frac{1}{\lambda} = \frac{1}{2\Gamma N} = \frac{1}{2}t_Q^{(M)}. \tag{29}$$

In the following, we are going to investigate whether the interaction with a stochastic field increases the coherence time of the cat according to the Wigner negativity criterion, and to check how the relation in Eq. (29) between t_W and t_Q is affected by the memory parameter γ.

The behaviour of the Wigner decoherence time is illustrated in Fig. 2. The upper left panel shows that t_W is significantly increased by the presence of time correlations in the

CSF (non-Markovian behavior), whereas the upper right panel reveals re-coherence effects for certain values of the detuning and memory parameters. In particular, the vertical black line ($\gamma = 0.05$) intercepts the solid red line ($\delta = 0.3$) just once, which means that revivals of nonclassicality displayed in the nonclassical depth criterion (see Fig.1) are not captured by the Wigner criterion. In the lower panel of Fig. 2 we compare t_Q and t_W by showing their ratio as a function of γ. For large values of the memory parameter γ (i.e. in the Markovian limit) the ratio approaches $\frac{1}{2}$, according to Eq. (29). In all the other cases, the ratio increases and approaches the limiting value $\frac{1}{\sqrt{2}}$ for $\gamma \to 0$. This may be understood as a consequence of the behaviour of $\sigma(t)$, as reported in Eqs. (21). Indeed, $\sigma(t)$ is basically linear in time for large γ, whereas it shows a quadratic behaviour for $\gamma \ll 1$.

The study of the Wigner negativity criterion in the off-resonance regime confirms the main conclusions we drew from the analysis of the nonclassical depth: for $\delta \neq 0$ the Schrödinger cat coherence survives longer and sudden death and birth of nonclassicality appear, which is expected by the analogy of the two considered criteria.

C. Vogel criterion

According to the Vogel criterion [17], which establishes a sufficient condition for nonclassicality, a state is nonclassical if there exist some complex numbers $\mu = (u, v)$ such that the normally ordered characteristic function satisfies

$$|\chi_1[\rho(t_V)](\mu)| > 1, \tag{30}$$

where $\chi_1[\rho(t)](\mu) = \chi_0[\rho(t)](\lambda) e^{e^{\frac{1}{2}|\mu|^2}}$. This is only a sufficient condition to characterize nonclassical states, but it has an advantage stemming from the fact that the symmetric characteristic function can be directly measured via balanced homodyne detection. The Vogel criterion is then suitable for an experimental implementation [89].

It is worth noticing, however, that in contrast with the two criteria shown previously, the Vogel criterion do depend on the state under investigation, i.e. the smallest interaction time t_V for which Eq. (30) is satisfied, depends on the amplitude α for the Schrödinger state or on the specific Fock state $|n\rangle$. Here, we consider cat states with real amplitude $\alpha = \alpha^* = \sqrt{2}$, the reason of this choice being justified later (see Section D). The Fock state $|n = 2\rangle$ is chosen such that the number of photons approximates the cat mean number of photons $\langle a^\dagger a\rangle \simeq 2$.

The plots in the left and right panels of Fig. 3, for cat and Fock states respectively, show the regions for which $|\chi_1[\rho(t_V)](\mu)| > 1$, as a function of $\mathrm{Re}(\mu) = u$ (with $v = 0$) and varying the detuning parameter δ (different colors). As it is possible to see in both figures, after a certain time t_V nonclassicality disappears, but the sudden birth and sudden death of quatumness is present also according to the Vogel criterion (look, for example, at the green and purple regions) and consistently with the two previous criteria, as far as the off-resonance interaction ($\delta \neq 0$) between the system and the CSF is set.

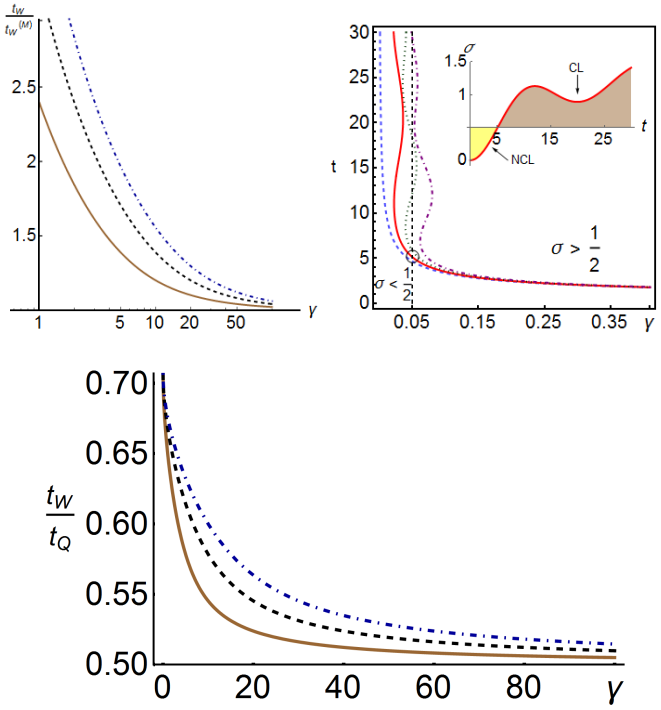

FIG. 2: (Color Online) Dynamics of quantumness according to the Wigner negativity criterion. Upper left panel: Wigner decoherence time t_W for a resonant interaction as a function of the memory parameter γ, for different values of coupling $\lambda = 1$ (solid brown), $\lambda = 2$ (dashed black) and $\lambda = 3$ (dot-dashed blue). For $\gamma \to \infty$, t_W approaches the Markovian limit $t_W^{(M)}$ independently on λ. Upper right panel: contour plots of $\sigma(t_W) = \frac{1}{2}$, in the off-resonance case, as a function of γ for a fixed value of the coupling $\lambda = 1$ and different values of the detuning $\delta = 0.3$ (solid red), $\delta = 0.4$ (dotted green) and $\delta = 0.5$ (dot-dashed purple). The dashed blue curve is chosen as a reference for the resonant case $\delta = 0$. In the regions lying to the left of the curves we have $\sigma(t) < \frac{1}{2}$, i.e. nonclassicality. The vertical line (dashed black) denotes points at fixed $\gamma = 0.05$ and the black circle indicates the solutions of $\sigma(t_W) = \frac{1}{2}$ for $\delta = 0.3$. Correspondingly, the regions of nonclassicality (NCL) and classicality (CL) are highlighted in the inset. Lower panel: the ratio t_W/t_Q as a function of γ with same values of λ as in the upper left panel. For $\gamma \gg 1$ the ratio approaches the Markovian value $\frac{1}{2}$, whereas for $\gamma \ll 1$ it approaches to the $\frac{1}{\sqrt{2}}$, due to the quadratic dependence on time of $\sigma(t)$.

D. Klyshko Criterion

In 1996, Klyshko introduced another criterion for nonclassicality, which is only sufficient [14], stating that if there exists an integer number n such that:

$$B(n) = (n+2)p(n)p(n+2) - (n+1)[p(n+1)]^2 < 0, \tag{31}$$

where $p(n) = \langle n|\rho(t)|n\rangle$ is the photon number probability, then the state ρ is nonclassical. Exactly as for the Vogel criterion, this nonclassicality witness is experimentally accessible as it is based on photon counting measurements. In our analysis of the Schrödinger cat nonclassicality, according to the Klyshko criterion, we found out that $B(1)$ becomes negative after a certain time t_K dependent on the detuning δ and

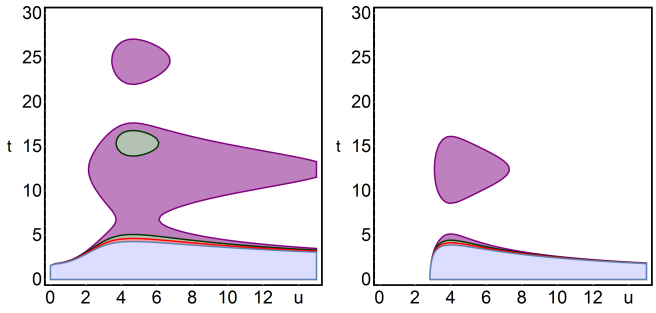

FIG. 3: (Color Online) Left panel: cat state Vogel time t_V as a function of u, with $|\alpha| = \sqrt{2}$. Right panel: Vogel time t_V as a function of u for Fock state $|2\rangle$. In both panels, $\gamma = 0.05$ and filled regions correspond to $|\chi_1[\rho(t_V)(u,0)| > 1$. From bottom to top: the blue region represents the resonant interaction ($\delta = 0$), whereas the red ($\delta = 0.3$), green ($\delta = 0.4$) and purple ($\delta = 0.5$) regions correspond to the off-resonance case. The spots for the green and the purple regions indicate the presence of revivals of nonclassicality.

the memory parameter γ. As it is shown in the left panel of Fig. 4, the Klyshko criterion confirms that the cat survival time increases for short γ and it is affected by detuning. Also in this case, sudden death and birth of quantumness can be observed, as for fixed γ there exist more than one time t_K that satisfies the Klyshko criterion (31). A similar behaviour is shown for the Fock state $|2\rangle$ in the right panel of Fig. 4, the only difference being the use of the quantity $B(0)$ instead of $B(1)$ to detect the quantum-to-classical transition. As we mentioned earlier, we have chosen $|\alpha| = \sqrt{2}$ for the cat. In turn, this choice maximizes the effectiveness of Klyshko criterion, i.e. is the value corresponding to the longest survival time by Klyshko criterion [25].

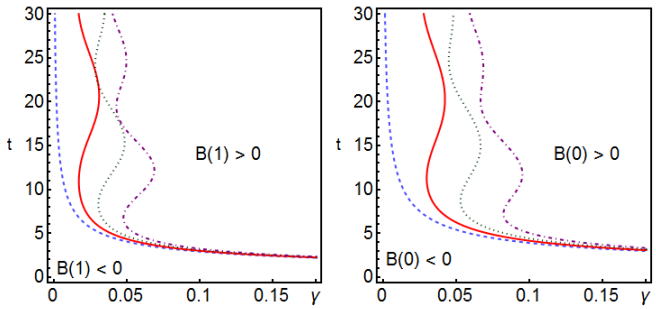

FIG. 4: (Color Online) Left panel: Dimensionless decoherence time t_K for the Klyshko criterion as a function of γ for the cat state with $\alpha = \sqrt{2}$. Right panel: Decoherence time t_K for the Klyshko criterion as a function of γ for the Fock state $|2\rangle$. In both panels, dashed blue curve represents the resonant interaction ($\delta = 0$), whereas solid red ($\delta = 0.3$), dashed green ($\delta = 0.4$) and dot-dashed purple ($\delta = 0.5$) curves refer to the off-resonance case. In the regions lying to the left of the curves we have $B(1) < 1$, i.e. nonclassicality.

E. A remark about decoherence times

In the previous Sections we went through a quantitative analysis of the nonclassicality dynamics of the Schrödinger cat and the Fock state, analyzing four different nonclassicality criteria. We described how the interaction of a quantized harmonic oscillator with a CSF, in terms of an OU process, allows to preserve the nonclassicality of each input state for certain periods of times and this result has been confirmed by each nonclassicality criteria. A quantitative analysis for both input states is shown in Table I, where we report the times corresponding to the sudden death of quantumness achieved according to the four considered criteria, for several values of the detuning δ. In particular, they are obtained by fixing the value of the parameter $\gamma = 0.05$, which is responsible of an appreciable memory effect in the considered OU process.

Schrödinger-cat state:

δ	0	0.3	0.4	0.5
t_Q	6.676	8.982	47.467	81.091
t_W	4.645	5.118	5.823	29.355
t_V	4.272	4.624	5.067	16.773
t_K	4.054	4.349	4.694	17.700

Fock (number) state:

δ	0	0.3	0.4	0.5
t_Q	6.676	8.982	47.467	81.091
t_W	4.645	5.118	5.823	29.355
t_V	3.886	4.140	4.425	5.128
t_K	5.412	6.253	21.329	49.527

TABLE I: Dimensionless decoherence times, obtained for $\gamma = 0.05$, $\lambda = 1$ and different values of the detuning δ, corresponding to the sudden death of quantumness of the evolved Schrödinger cat state (Upper Table) and the evolved Fock state (Lower Table), according to the four nonclassicality criteria: nonclassical depth (t_Q), Wigner negativity (t_W), Vogel criterion (t_V) and Klyshko criterion (t_K).

We notice that the times estimated with the Vogel criterion (or the Klyshko criterion) are always shorter than the nonclassical depth and the Wigner negativity decoherence times. This is consistent with the fact that Vogel and Klyshko criteria provide only sufficient conditions for the loss of quantumness. Indeed, it is possible to still have an amount of nonclassicality in the evolving state which is undetected by these two criteria. Actually, Diosi demonstrated that for some nonclassical states the Vogel criterion is not satisfied [90]. In other words, the evolved cat or Fock state may still show some quantumness, according to other nonclassicality criteria, while the Vogel criterion is no longer violated.

F. Input-output fidelity

The presence of oscillations in the dynamics of nonclassicality suggests that some form of information backflow from the environment to the system is taking place. This phenomenon is usually associated to quantum non-Markovianity and we want to explore this connection, at least in a qualitative way. In fact, the markovian character of the quantum map (18) for a coherent input state may be easily proved [58],

but Markovianity on coherent states does not necessarily imply Markovianity on Fock states or superposition of coherent states.

The non-Gaussian character of the channel under investigation prevents the analytic evaluation of non Markovianity measures based on fidelity [58] or the Fisher information [57]. On the other hand, since the dynamics induced by the interaction with the CSF is fully described by the quantum channel (18), the input-output fidelity, assessing the dissimilarity between the input state and the output state of a quantum map, may be evaluated in a straightforward way as

$$F_{IO} = \langle\psi|\mathcal{E}(\rho)|\psi\rangle\,, \tag{32}$$

where ψ is the initial state, assumed to be a pure state.

Actually, a non monotonous time evolution of F_{IO} cannot be, in general, interpreted as a signature of backflow of information from the environment to the system (one may construct examples where a system interact with a markovian environment and still the IO fidelity oscillates due to some unitary terms in the interaction Hamiltonian). On the other hand, we found that for our system F_{IO} provides useful information which may be relevant in the qualitative and quantitative characterization of non-Markovianity.

The F_{IO}s for a cat state and a Fock state interacting with a classical environment are given by

$$F_{IO}^{(cat)}(t) = \frac{1 + 4e^{2|\alpha|^2} + e^{4|\alpha|^2} + e^{\frac{4|\alpha|^2}{1+\sigma(t)}} + e^{\frac{4\sigma(t)|\alpha|^2}{1+\sigma(t)}}}{2[1+\sigma(t)]\left[1+e^{2|\alpha|^2}\right]^2}\,, \tag{33}$$

$$F_{IO}^{(Fock)}(t) = \frac{1}{\sqrt{\pi}(1+\sigma(t))}\frac{\Gamma(n+\frac{1}{2})}{\Gamma(n+1)}\times \\ \times\, {}_2F_1\left(-n, \frac{1}{2}, \frac{1}{2}-n, \left[\frac{1-\sigma(t)}{1+\sigma(t)}\right]^2\right) \tag{34}$$

where ${}_2F_1(a,b,c,;x)$ is a hypergeometric function. The behaviour of the IO fidelities in Eqs. (33) and (34) as a function of the interaction time is reported in the upper panels of Fig. 5 for $\alpha = \sqrt{2}$ and $n = 2$.

For zero detuning, the IO fidelities show a monotonous behaviour with the memory parameter γ, which determines how fast the F_{IO}s decrease. This corresponds to a decoherence dynamics where the state evolves loosing memory of its initial conditions. Conversely, in the presence of detuning the nonresonant curves detach from the respective resonant ones and F_{IO}s show a non monotonous behaviour where the state goes back to the initial preparation, at least partially. Notice that the input-output fidelities of the cat and the Fock states shows a similar behavior, even though they are quantitatively different. In both cases, the oscillating behaviour is present for values of γ up to a threshold γ^*, which depends on the value of the other parameters λ, and δ and *do not* depend on the initial state, i.e. it represents a property of the channel. For $\lambda = 1$ and $\delta = 0.3$ (see Fig. 5) we have $\gamma^* \simeq 0.082$. Loosely speaking, the existence of the threshold parameter γ^* means that the evolution is monotonous as far as the time correlations of the environment are weak enough. Remarkably, the

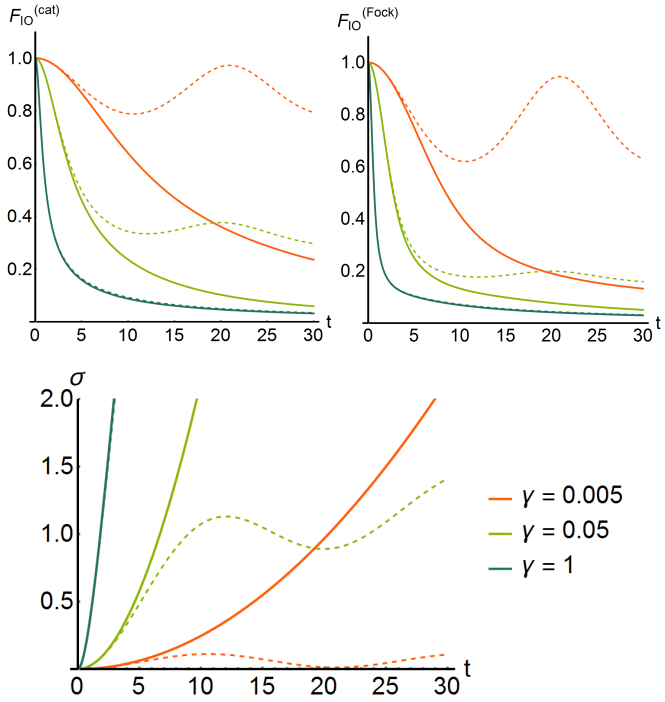

FIG. 5: (Color Online) Input-output fidelity as a function of the interaction time for a cat state with $\alpha = \sqrt{2}$ (upper-left panel) and a Fock state with $n = 2$ (upper-right panel) for different values of the memory parameter γ and the detuning δ and for fixed coupling $\lambda = 1$. For comparison, the behaviour of the variance σ (lower panel) in the same conditions. In all the panels the orange curves are for $\gamma = 0.005$, green is for $\gamma = 0.05$, and blue refers to $\gamma = 1$ (blue). The solid curves correspond to zero detuning (resonant case) and the dashed ones are for $\delta = 0.3$.

same kind of transition may be also seen in the time dependence of the variance $\sigma(t)$. As it is apparent from the lower panel of Fig. 5, the presence of revivals in the behaviour of σ also depends on the value of the memory parameter γ and it may be proven numerically that also the revivals disappear when $\gamma \gtrsim \gamma^*$. Overall, this confirms the backflow of information and the ability of the input-output fidelity to capture this feature of the quantum channel.

IV. POWER-LAW PROCESS

As mentioned in the introduction, the main conclusions of our analysis are qualitatively independent on the nature of the CSF used to model the environment. In order to show this explicitly, and to briefly illustrate the quantitative effects of a differrent modelling, we report here the results obtained for a Gaussian process characterized by a long range power-law autocorrelation function of the form:

$$K(t_1,t_2) = \frac{\beta-1}{2}\frac{\gamma\lambda}{(1+\gamma|t_1-t_2|)^\beta} \tag{35}$$

where $\beta > 2$. The attention will be focused on the nonclassical depth criterion, as it is the most relevant one. The explicit

form of $\sigma(t)$ for the power-law process in the case of the resonant interaction ($\delta = 0$) is the following:

$$\sigma(t) = \lambda t + \lambda \frac{(1+\gamma t)^{2-\beta} - 1}{\gamma(\beta - 2)}. \quad (36)$$

This expression can be approximated in some particular regimes to:

$$\sigma(t) \simeq \lambda t + \frac{\lambda \gamma t^2}{(\beta-2)(1+\gamma t)^{\beta}} \quad (\gamma \gg 1) \quad (37)$$

$$\sigma(t) \simeq \frac{\lambda t^2}{2}(\beta - 1) \quad (\gamma \ll 1). \quad (38)$$

As we can see from (37), for $\gamma \to \infty$ the nonclassical depth time approaches the Markovian limit $\sigma(t) \propto t$. Also for the power-law process γ plays the role of a memory parameter.

In the nonresonant case, the analytic form of $\sigma(t)$ is extremely complex and is not reported in this paper, whereas the results are explained in the following. The presence of sudden death and sudden birth of quantumness for the nonresonant interaction is shown, for an initial cat state, in the left panel of Fig. 6, where, for fixed γ and different choices of the detuning parameter $\delta \neq 0$, we can see more than one value of time t_Q for which the nonclassical depth criterion is satisfied. In the right panel of Fig. 6 we show the nonclassical depth time as a function of the parameter β of power-law autocorrelation function. Furthermore, the presence of sudden death and birth of nonclassicality depends not only on the particular combination of parameters (δ, γ), but also on the parameter β itself. Actually, Fig. 6 shows that nonclassicality revivals can be also observed for the power-law process just like for the OU process, and that this phenomenon is mostly due to the introduction of the detuning parameter.

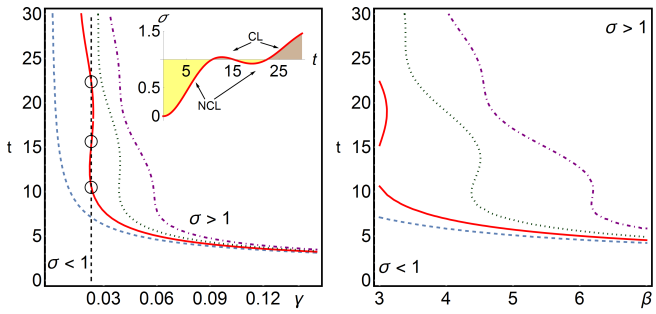

FIG. 6: (Color online) Dynamics of quantumness according to the nonclassical depth criterion for a cat states evolving in classical environment with power-law autocorrelation function. In both panels, the dashed blue curve represents the resonant case $\delta = 0$, whereas solid red ($\delta = 0.3$), dotted green ($\delta = 0.4$), dot-dashed purple ($\delta = 0.5$) curves refer to the off-resonance case. Left panel: nonclassical depth time t_Q as a function of γ in the case of a Gaussian power-law process, for fixed $\beta = 3$ and $\lambda = 1$. For $\gamma \gg 1$ the nonclassical depth time t_Q approaches the Markovian limit independently of δ. Sudden death and birth of quantumness are highlighted by the circles along the dashed black line at $\gamma = 0.023$ and, correspondingly, in the inset. Right panel: nonclassical depth time t_Q as a function of β and fixed $\gamma = 0.023$.

V. CONCLUSIONS

In this paper we have investigated the quantum-to-classical transition for an harmonic oscillator initially prepared in a maximally nonclassical state and then interacting with a classical fluctuating field. As a first result, we have shown that modeling the environment by means of classical stochastic fields allows to properly describe the decoherence process in the presence of memory effects, without resorting to approximated quantum master equations. In particular, we have been able to introduce non-Markovian effects in a controlled way and to recover the Markovian behavior by a suitable set of limiting values of the parameters.

Our results show that the presence of classical memory in the environment strongly influences the decoherence time, increasing the survival time of nonclassicality and leading to dynamical sudden death and birth of quantumness. In particular, when the environment spectrum contains the natural frequency of the oscillator we observe an increase of the survival time compared to the Markovian case whereas, in the presence of a detuning, we see the occurrence of sudden death and sudden birth of quantumness, as indicated by collapses and revivals of nonclassicality. In order to address this phenomena quantitatively, we have analyzed the behavior of four different criteria introduced to witness nonclassicality, also relating them to experimentally observable quantities. All this quantifiers agree in describing the nontrivial decoherence process and the revivals of nonclassicality, thus supporting the validity of our model and the main conclusions of our analysis, which may be summarized as follows: i) classical memory effects increase the survival time of quantumness; ii) a detuning between the natural frequency of the system and the central frequency of the environment produces revivals of quantumness.

Acknowledgments

This work has been supported by MIUR (FIRB "LiCHIS" RBFR10YQ3H). MGAP thanks C. Benedetti, M. G. Genoni and M. A. C. Rossi for discussions.

Appendix A

The s-ordered characteristic function of the cat state is given by

$$\chi_s[\mathrm{cat}](\mu) = \frac{2}{\mathcal{N}} e^{-\frac{1}{2}(1-s)|\mu|^2} \times \left[\cos\left(2\,\mathrm{Im}\,\mu\alpha^*\right) + e^{-2|\alpha|^2}\cosh\left(2\,\mathrm{Re}\,\mu\alpha^*\right)\right] \quad (A1)$$

The s-ordered Wigner function of the cat state is given by

$$W_s[\mathrm{cat}](\beta) = \frac{2\, e^{-\frac{2|\beta|^2}{1-s}}}{\mathcal{N}\pi(1-s)} \times \left[\exp\left\{ \frac{2s|\alpha|^2}{1-s} \right\} \cos\left(\frac{4}{1-s} \operatorname{Re} \beta\alpha^* \right) + \exp\left\{ -\frac{2|\alpha|^2}{1-s} \right\} \cosh\left(\frac{4}{1-s} \operatorname{Im} \beta\alpha^* \right) \right]. \quad \text{(A2)}$$

The matrix elements of the Schrödinger state in the Fock states basis are given by

$$\rho_{n,m} = \frac{1}{\mathcal{N}} e^{-|\alpha|^2} \frac{\alpha^n (\alpha^*)^m}{\sqrt{n!m!}} [1 + (-1)^n][1 + (-1)^m]. \quad \text{(A3)}$$

The s-ordered characteristic function of the Fock state is given by

$$\chi_s[n](\mu) = \exp\left\{ -\frac{(1-s)|\mu|^2}{2} L_n(|\mu|^2) \right\}, \quad \text{(A4)}$$

where $L_n(x)$ is the Laguerre polynomial of order n.

The s-ordered Wigner function of the Fock state is given by

$$W_s[n](\beta) = (-1)^n \frac{2}{\pi(1-s)} \left(\frac{1+s}{1-s} \right)^n \times \exp\left\{ -\frac{2|\beta|^2}{1-s} \right\} L_n\left(\frac{4|\beta|^2}{1-s^2} \right). \quad \text{(A5)}$$

[1] S. Haroche and J.-M. Raimond, *Exploring the Quantum*, (Oxford University Press 2006).
[2] W. H. Zurek, Physics Today **44**(10), 36 (1991).
[3] J. P. Paz, S. Habib, and W. H. Zurek, Phys. Rev. D **47**, 488 (1993).
[4] A. Kossakowski, Rep. Math. Phys. **3**, 247 (1972).
[5] V. Gorini, A. Kossakowski, and E. C. G. Sudarshan, J. Math. Phys. **17**, 821 (1976).
[6] G. Lindblad, Commun. Math. Phys. **48**, 119 (1976)
[7] T. Banks, L. Susskind, and M. E. Peskin, Nucl. Phys. B **244**, 125 (1984).
[8] H. Carmichael, *An Open Systems Approach to Quantum Optics*, (Springer-Verlag Berlin Heidelberg, 1993).
[9] H. P. Breuer and F. Petruccione, *The Theory of Open Quantum Systems* (Oxford University Press, Oxford, 2002).
[10] U. Weiss, *Quantum Dissipative Systems* (3rd Edition), (World Scientific, Singapore, 2008).
[11] R. J. Glauber, Phys. Rev. **131**, 2766 (1963).
[12] E. C. G. Sudarshan, Phys. Rev. Lett. **10**, 277 (1963).
[13] K. E. Cahill, R. J. Glauber, Phys. Rev. **177**, 1882 (1969).
[14] D. N. Klyshko, Phys. Lett. A **213**, 7 (1996).
[15] M. Takeoka, M. Ban, M. Sasaki, J. Opt. B **4** 114 (2002).
[16] R. Egger, H. Grabert, and U. Weiss, Phys. Rev. E **55**, R3809 (1997).
[17] W. Vogel, Phys. Rev. Lett. **84**, 1849 (2000).
[18] Th. Richter and W. Vogel, Phys. Rev. Lett. **89**, 283601 (2002).
[19] A. Kenfack, K. Zyczkowski, J. Opt. B **6**, 396 (2004).
[20] C. T. Lee, Phys. Rev. A **44**, R2775 (1991).
[21] N. Lutkenhaus, S. M. Barnett, Phys. Rev. A **51**, 3340 (1995).
[22] J. K. Korbicz, J. I. Cirac, J. Wehr, and M. Lewenstein, Phys. Rev. Lett. **94**, 153601 (2005).
[23] J. K. Asbóth, J. Calsamiglia, and H. Ritsch, Phys. Rev. Lett. **94**, 173602 (2005).
[24] T. Kiesel, W. Vogel, V. Parigi, A. Zavatta and M. Bellini, Phys. Rev. A **78**, 021804R (2008).
[25] J. Paavola, M. J. Hall, M. G. A. Paris, S. Maniscalco, Phys. Rev. A **84**, 012121 (2011).
[26] I. P. Degiovanni, M. Genovese, V. Schettini, M. Bondani, A. Andreoni, M. G. A. Paris, Phys. Rev. A **79**, 063836 (2009).
[27] A. Miranowicz, M. Bartkowiak, X. Wang, Y. X. Liu, and F. Nori Phys. Rev. A **82**, 013824 (2010).
[28] J. Solomon Ivan, S. Chaturvedi, E. Ercolessi, G. Marmo, G. Morandi, N. Mukunda, and R. Simon, Phys. Rev. A **83**, 032118 (2011).
[29] G. Brida, M. Bondani, I. P. Degiovanni, M. Genovese, M. G. A. Paris, I. Ruo Berchera, and V. Schettini, Found. Phys. **41**, 305 (2011).
[30] A. Serafini, M. G. A. Paris, F. Illuminati, and S. De Siena, J. Opt. B **7**, 19 (2005).
[31] A. Serafini, S. De Siena, F. Illuminati, and M. G. A. Paris, J. Opt. B **6**, 591 (2004).
[32] M. G. A. Paris, Phys. Lett. A **225**, 28 (1997).
[33] M. G. A. Paris, Phys. Rev. A. **62**, 033813 (2000).
[34] M. S. Kim, W. Son, V. Buzek, and P. L. Knight, Phys. Rev. A **65**, 032323 (2002).
[35] W. Xiang-bin, Phys. Rev. A **66**, 024303 (2002).
[36] S. Olivares, M. G. A. Paris, Phys. Rev. Lett **107**, 170505 (2011).
[37] A. Ferraro, M. G. A. Paris, Phys. Rev. Lett **108**, 260403 (2012).
[38] S. Maniscalco and F. Petruccione. Phys. Rev. A **73**, 012111 (2006).
[39] X.-T. Liang. Phys. Rev. E **82**, 051918 (2010).
[40] P. Rebentrost and A. Aspuru-Guzik. J. Chem. Phys. **134**, 101103 (2011).
[41] A. Chiuri, C. Greganti, L. Mazzola, M. Paternostro, P. Mataloni, Scient. Rep. **2**, 968 (2012).
[42] B-H. Liu, L. Li, Y-F. Huang, C-F. Li, G-C. Guo, E-M. Laine, H-P. Breuer, J. Piilo, Nat. Phys. **7**, 931 (2011).
[43] A. Smirne, D. Brivio, S. Cialdi, B. Vacchini, M. G. A. Paris, Phys. Rev. A **84**, 032112 (2011).
[44] J. Piilo, S. Maniscalco, K. Harkonen, and K.-A. Suominen, Phys. Rev. Lett. **100**, 180402 (2008).
[45] A. Smirne, S. Cialdi, G. Anelli, M. G. A. Paris, B. Vacchini, Phys. Rev. A **88**, 012108 (2013).
[46] S. Maniscalco, S. Olivares, M. G. A. Paris, Phys. Rev. A **75**, 062119 (2007).
[47] J. Anders, Phys. Rev. A **77**, 062102 (2008).
[48] J. P. Paz, A. J. Roncaglia, Phys. Rev. A **79**, 032102 (2009).
[49] R. Vasile, S. Olivares, M. G. A. Paris, S. Maniscalco, Phys. Rev. A **80**, 062324 (2009).
[50] R. Vasile, S. Olivares, P. Giorda, M. G. A. Paris, S.Maniscalco, Phys. Rev. A **82**, 012312 (2010)
[51] F. Galve, G. L. Giorgi, and R. Zambrini, Phys. Rev. A **81**,

062117 (2010) .
[52] L. A. Correa, A. A. Valido, D. Alonso, Phys. Rev. A **86**, 012110 (2012).
[53] A. Cazzaniga, S. Maniscalco, S. Olivares, M. G. A. Paris, Phys. Rev. A **88**, 032121 (2013).
[54] V. Venkataraman, A. D. K. Plato, T. Tufarelli, M. S. Kim J. Phys. B. **47**, 015501 (2014).
[55] H.-P. Breuer, E.-M. Laine, and J. Piilo, Phys. Rev. Lett. **103**, 210401 (2009).
[56] A. Rivas, S. Huelga, M. B. Plenio, Phys. Rev. Lett. **105**, 050403 (2010).
[57] X-M. Lu, X. Wang, C. P. Sun, Phys. Rev. A **82**, 042103 (2010).
[58] R. Vasile, S. Maniscalco, M. G. A. Paris, H.-P. Breuer, J. Piilo, Phys. Rev. A **84**, 052118 (2011).
[59] D. Chruściński, S. Maniscalco, Phys. Rev. Lett. **112**, 120404 (2014)
[60] R. Vasile, S. Olivares, M. G. A. Paris, S. Maniscalco Phys. Rev. A **83**, 042321 (2011).
[61] A. W. Chin, S. F. Huelga, M. B. Plenio, Phys. Rev. Lett. **109**, 233601 (2012).
[62] B. Bylicka, D. Chruściński, S. Maniscalco Scient. Rep. **4**, 5720 (2014).
[63] J. Helm and W. T. Strunz, Phys. Rev. A **80**, 042108 (2009).
[64] J. Helm, W. T. Strunz, S. Rietzler, and L. E. Würflinger, Phys. Rev. A **83**, 042103 (2011).
[65] D. Crow, R. Joynt, Phys. Rev. A **89**, 042123 (2014).
[66] W. M. Witzel, K. Young, S. Das Sarma, Phys. Rev. B **90**, 115431 (2014).
[67] O. Astafiev, Yu. A. Pashkin, Y. Nakamura, T. Yamamoto, and J. S. Tsai, Phys. Rev. Lett. **93**, 267007 (2004).
[68] Y. M. Galperin, B. L. Altshuler, J. Bergli, and D. V. Shantsev, Phys. Rev. Lett. **96**, 097009 (2006).
[69] B. Abel and F. Marquardt, Phys. Rev. B **78**, 201302(R) (2008).
[70] C. W. Gardiner, *Handbook of Stochastic Methods*, (Springer-Verlag, Berlin, 1983).
[71] E. Paladino, L. Faoro, G. Falci, and R. Fazio, Phys. Rev. Lett. **88**, 228304 (2002).
[72] L. Cywiński, R. M. Lutchyn, C. P. Nave, and S. Das Sarma, Phys. Rev. B **77**, 174509 (2008).
[73] C. Benedetti, F. Buscemi, P. Bordone, M. G. A. Paris, Int. J. Quantum Inf. **10**, 1241005 (2012).
[74] H. J. Wold, H. Brox, Y. M. Galperin, J. Bergli Phys. Rev. B **86**, 205404 (2012)
[75] C. Benedetti, F. Buscemi, P. Bordone, M. G. A. Paris, Phys. Rev. A **87**, 052328 (2013).
[76] J.-T. Hung, L. Cywiǹski, X. Hu, S. Das Sarma, Phys. Rev. B **88**, 085314 (2013).
[77] E. Paladino, Y. M. Galperin, G. Falci, B. L. Altshuler, Rev. Mod. Phys. **86**, 361 (2014).
[78] C. Benedetti, M. G. A. Paris, S. Maniscalco, Phys. Rev. A **89**, 012114 (2014).
[79] C. Benedetti and M. G. A. Paris, Int. J. Quantum Inf. **12**, 1461004 (2014).
[80] M. A. C. Rossi, C. Benedetti, M. G. A. Paris, Int. J. Quantum Inf. **13**, 1560003 (2015)
[81] R. L. Hudson, Rep. Math. Phys. **6**, 249 (1974).
[82] G. E. Uhlenbeck and L. S. Ornstein, Phys. Rev. **36**, 823 (1930).
[83] R. R. Puri, *Mathematical methods of quantum Optics*, (Springer, Berlin, 2001).
[84] W. Magnus, Comm. Pure and Appl. Math. **7**, 649 (1954).
[85] S. Blanes, F. Casas, J.A. Oteo, and J. Ros, Phys. Rep. **470**, 151 (2008).
[86] O. Cohen, Phys. Rev. A **56**, 3484 (1997).
[87] K. Banaszek, K. Wodkiewicz, Phys. Rev. A **58**, 4345 (1998).
[88] A. S. Holevo, Probl. Peredachi Inf., **9**, 3 (1973).
[89] I. Lvovsky, J. H. Shapiro, Phys. Rev. A **65**, 033830 (2002).
[90] L. Diósi, Phys. Rev. Lett. **85**, 2841 (2000).